THE ASTROPHYSICAL JOURNAL, 463:158–168, 1996 May 20

X-RAY SPECTRAL VARIABILITY IN NGC 7469

KAREN LEIGHLY[1]
NASA/Goddard Space Flight Center, Greenbelt, MD, 20771
HIDEYO KUNIEDA
Department of Physics, Nagoya University, Nagoya 464, Japan
HISAMITSU AWAKI
Department of Physics, Kyoto University, Kyoto 606, Japan
AND
SACHIKO TSURUTA
Department of Physics, Montana State University, Bozeman, MT 59717
Received 1994 July 27; accepted 1995 December 1

ABSTRACT

We present analyses of two *Ginga* observations and two observations from the *ROSAT* database of NGC 7469, focusing on the spectral variability observed on timescales of days and longer. During the 3 day 1988 *Ginga* observation, the hardness ratio (8–21 keV/3.4–5.7 keV) increased significantly as the total flux decreased by 30%. As the spectrum is well fit by the reflection model and since the spectral variability dominates the higher energy band, this could be explained by either a variation in the power-law index or in the effective covering fraction of the reflecting material. This ambiguity is inherent in reflection modeling of *Ginga* spectra from moderate flux Seyfert 1 galaxies. Assuming that the power-law index did not change, we find that the reflected flux is consistent with being constant, suggesting that much of the reflecting material may be located more than 3 light-days from the continuum source with the molecular torus being a plausible site. This scenario is also supported by the report of a narrow rather than broad iron Kα line in the *ASCA* data by Guainazzi et al. NGC 7469 was faint during the 1989 *Ginga* observation, but variability was observed with doubling timescale of 5 hr, and the spectrum was harder. A reflection component could not be constrained, and the change in the spectrum could be explained by an increase in neutral absorption.

The brighter of two *ROSAT* spectra was significantly softer, and in both spectra there was evidence of spectral complexity, as has been previously reported by Turner, George, & Mushotzky and Brandt et al. The spectrum could be fit by a variety of two-component models, including a warm absorber model, an ionized disk model, and a thermal model with single-component blackbody spectrum, but joint fitting of the 1988 average *Ginga* spectrum and the nonsimultaneous *ROSAT* spectra favored thermal models, as other models required an anomalously high reflection ratio. This model is supported by the observation of a soft excess component and the lack of ionized absorption edges in the *ASCA* spectrum by Guainazzi et al. The long-term spectral variability could be explained by relative variability between the power-law and soft excess component normalizations, perhaps implying that hard X-ray reprocessing in thermal material does not dominate on long timescales.

Subject headings: galaxies: individual (NGC 7469) — galaxies: Seyfert — X-rays: galaxies

1. INTRODUCTION

NGC 7469 is a moderate-luminosity ($L_{2-10} \sim 3 \times 10^{43}$ ergs s^{-1}) Seyfert 1 galaxy, first detected in X-rays using *Uhuru* (Forman et al. 1978). Subsequent observations discovered rapid, large-amplitude flux variability including an observation by *Ariel 5* of a 2 day flare in which the flux increased by a factor of 6 (Marshall, Warwick, & Pounds 1981). Rapid variability by a factor of 2 in 5 hr was observed in the 1–7 keV X-rays with no accompanying variability of the 0.05–2 keV X-rays during one *EXOSAT* observation, while variability in both bands occurred among four observations in 10 days (Barr 1986).

Evidence for a soft excess component has been found often. When the *EXOSAT* spectra were fitted with an absorbed power-law model, the absorption column was found to be below the Galactic value, implying the presence of a soft excess component (Barr 1986). A soft excess component was also found in the *Einstein* IPC + MPC spectra (Urry et al. 1989) and SSS + MPC spectra (Turner et al. 1991). *ROSAT* spectra showed evidence for soft spectral complexity (Turner, George, & Mushotzky 1993a; Brandt et al. 1993). A soft excess component was also found in the 1993 *ASCA* spectrum (Guainazzi et al. 1994). Considering all the *EXOSAT* data, Grandi et al. (1992) found that the spectrum became flatter as the flux increased. Walter & Courvoisier (1992) also analyzed the *EXOSAT* spectra and found that they were consistent with a constant soft X-ray component. Evidence for hard X-ray reprocessing has been found including a hard reflection component and an iron line in the 1988 averaged *Ginga* spectrum (Piro, Yamauchi, & Matsuoka 1990), which was found to be narrow in the *ASCA* spectra (Guainazzi et al. 1994). Evidence for an iron line was found in the *EXOSAT* Spectral Survey sample, at the 97.5% confidence level (Leighly, Pounds, & Turner 1989). Strong evidence for a reflection component was also found in the *HEAO 1* A-2 data (Weaver, Arnaud, & Mushotzky 1995).

In this paper we investigate the spectral variability in the *ROSAT* and *Ginga* data. In § 2 the data, reduction, and

[1] Current address: RIKEN, Institute of Physical and Chemical Research, Hirosawa 2-1, Wakoshi, Saitama 351-01, Japan.

timing analyses are described including hardness ratios, which clearly demonstrate the presence of spectral variability. Section 3 gives the spectral fitting results which are used to determine which component likely varies producing the observed spectral variability. In § 4 these results are discussed in terms of current physical models of active galactic nuclei (AGN).

2. DATA

2.1. *The Ginga Data*

The *Ginga* mission and Large Area Counter (LAC) are described in Turner et al. (1989). Conservative selection criteria were used (COR > 9, counting rate above the upper discriminator less than 5.95 counts per detector, and earth elevation angle greater than 6°). The shape of background spectrum, particularly in low energies, varies as a function of the ascending node of the satellite due to radioactive decay (e.g., Hayashida et al. 1989), and this can result in spurious spectral variability. We employed additional conservative selection criteria in order to minimize possible systematic errors. The data were selected further so that the same range (within 300°–180°) of ascending node was represented in the source and background data. Furthermore, spectral variability was investigated for timescales no shorter than 1 day, over which the effect of the main component of the variable background shape is expected to average out. Remaining background and source data were sorted and subtracted according to the count rate above the upper discriminator. Only data from the top layer of the LAC detector were used for spectral fitting because of general overall better statistics. Details of *Ginga* data selection and this background subtraction method, commonly used at Nagoya University and RIKEN in Japan, can be found in the Appendix of Leighly et al. (1994). Further discussion of the reliability of this method is given in Matsuoka et al. (1990), and a discussion of the effect of this background subtraction method on spectral variability investigations is given in Fiore et al. (1992).

NGC 7469 was first observed for 3 days in 1988 from July 10 through July 13, and source-free sky was observed for 2 days during 1988 July 8 and 9. The total flux light curve (1.1–20.9 keV) is shown in the top panel of Figure 1*a*, where the zero reference is 1988 July 10 1:11:59.509. During the first day, the average flux (top plus midlayer) was about 24 counts s^{-1}, but it decreased after 2.2 days to an average of about 18 counts s^{-1}.

Spectral variability occurred during this observation. The hardness ratio computed from the top plus midlayer data (8.0–20.9/3.4–5.7 keV), shown in the second panel of Figure 1*a*, demonstrates that the hardness is variable on the timescale of days with the spectrum hardening as the flux decreased, opposite the *EXOSAT* result (Grandi et al. 1992). The softness ratio (1.1–3.4/3.4–5.7 keV) varies also, but with much less significance. Comparing the average ratio for the first day with the average ratio for the second and third days shows a reduced χ^2 for the constant model of 2.3 for the softness but 10 for the hardness ratios.

A second observation was made on 1989 November 23–24, with nearby blank sky being observed on 1989 November 22. The light curve from the 1989 observation is shown in Figure 1*b*, where the zero reference point is 1989 November 23 19:11:6. Satellite attitude problems occurred during this observation, with the transmission decreasing from ~0.78 from the beginning of each day, so that before aspect correction the average flux was about 5 counts s^{-1}. For spectral analysis, only data with collimator transmission >0.6 were used as marked in Figure 1*b*. During the second day, the flux decreased by about 40% in 20,000 s. This decrease is consistent with the factor of 2 decrease in 5–6 hr observed using *EXOSAT* (Barr 1986). The hardness ratio in the lower panel shows that no spectral variability occurred during this observation, but the spectrum is significantly harder than was observed in 1988.

2.2. *The ROSAT Data*

Two on-axis *ROSAT* observations of NGC 7469 were available in the archive. The source spectrum extraction

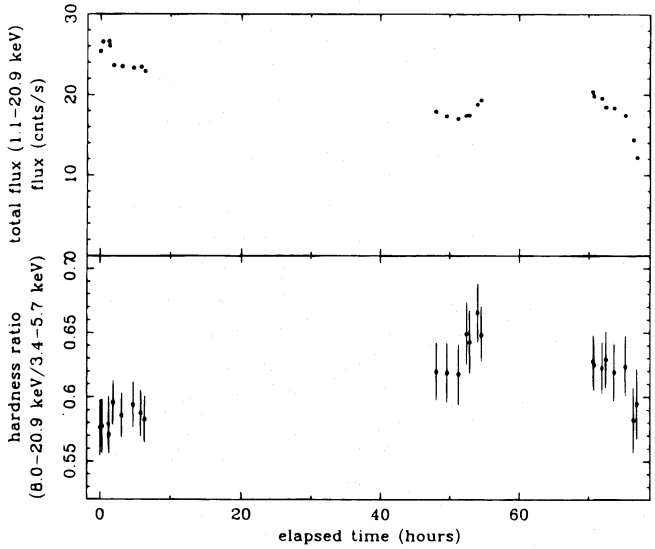

FIG. 1*a*

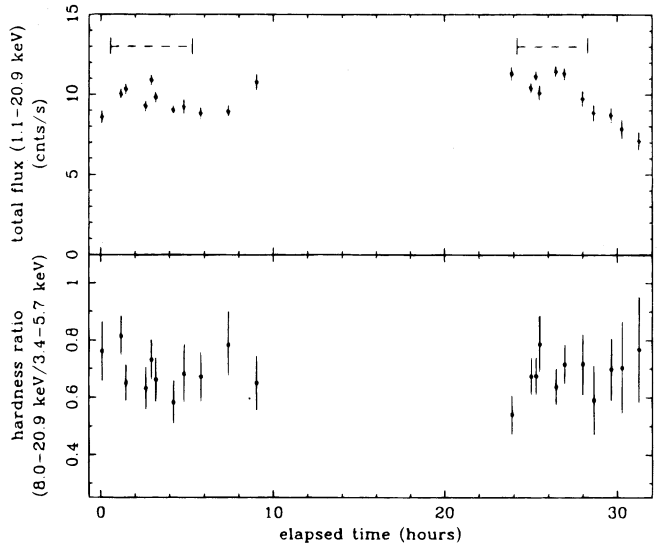

FIG. 1*b*

FIG. 1.—*Ginga* light curves, where the top panel shows the 1.1–20.9 keV total flux and the bottom panel shows the 8.00–20.9 keV/3.3–5.7 keV hardness ratio light curves, respectively. (*a*) *Ginga* 1988 observation; note the general trend of increasing hardness with decreasing flux. (*b*) *Ginga* 1989 observation; note the decrease in flux during the last part of the second day of observation. The marked intervals show the data accumulated for spectral analysis corresponding to transmission $T > 0.6$.

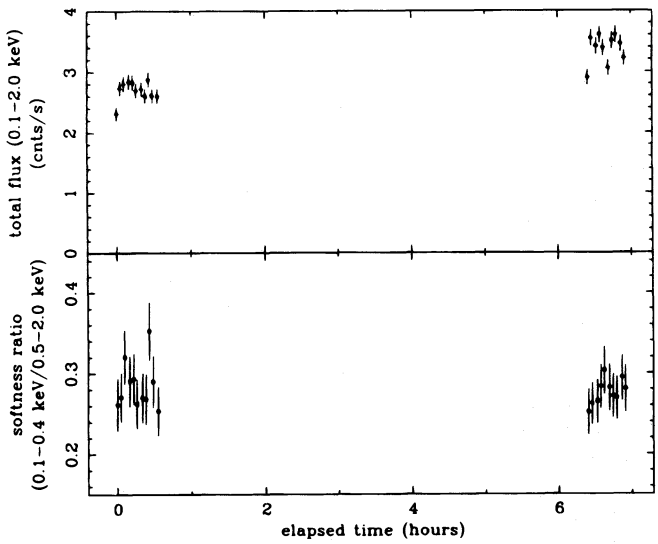

FIG. 2a

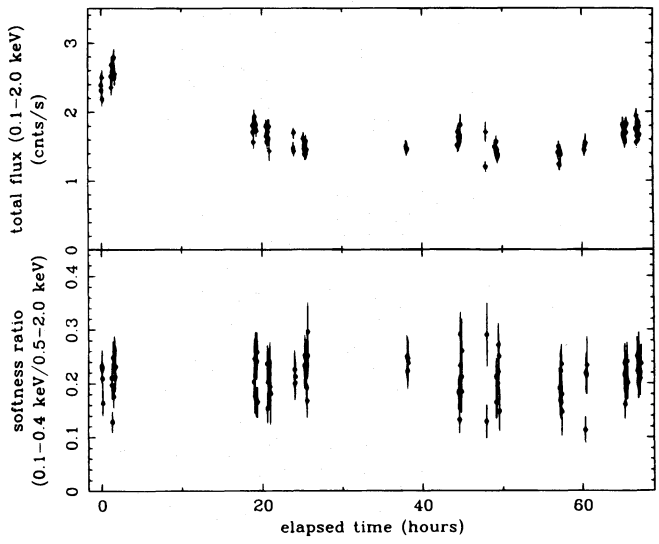

FIG. 2b

FIG. 2.—*ROSAT* light curves, where the top panels show the 0.1–2 keV total flux and the bottom panels show the 0.1–0.4 keV/0.5–2.0 keV softness ratio light curves, respectively. Significant flux variability but no significant spectral variability was observed on timescales of 1 day, with the higher flux 1991 observation showing a larger softness ratio. (*a*) *ROSAT* 1991 observation; (*b*) 1992 *ROSAT* observation.

radius used was 3′.2, and background was taken from an annulus. The "gain2" detector response matrix was used for spectral fitting as recommended for observations occurring after 1991 October. We are aware of the remaining calibration uncertainties of the *ROSAT* PSPC which are discussed in detail by Brinkmann et al. (1994) and Fiore et al. (1994). The possible effect of this residual uncertainty on the observed spectral variability is discussed in § 3.2.

NGC 7469 was observed on 1991 November 28 for 4251 s, and the mean flux was 3.0 counts s^{-1}. The light curve in Figure 2*a* shows that between the two observation intervals the source flux increased by ~25%. Spectral fitting results from this observation were reported previously by Turner et al. (1993a), and differences between those results and these are probably attributable to the use of the updated detector response matrix. NGC 7469 was also observed using *ROSAT* from 1992 May 28 to 1992 May 31 for 18,575 s. The average flux from this observation was 1.72 counts s^{-1}. The light curve shown in Figure 2*b* demonstrates that a 40% decrease in flux occurred during the observation. Spectral fitting results from this observation were reported by Brandt et al. (1993). The softness ratios (0.1–0.4 keV/0.5–2.0 keV) show that there is no significant spectral variability during either observation. However, the pulse-height analyzer (PHA) ratio given in Figure 3 shows that the spectrum hardened, particularly below 0.5 keV, as the flux decreased between the two observations spaced 6 months apart.

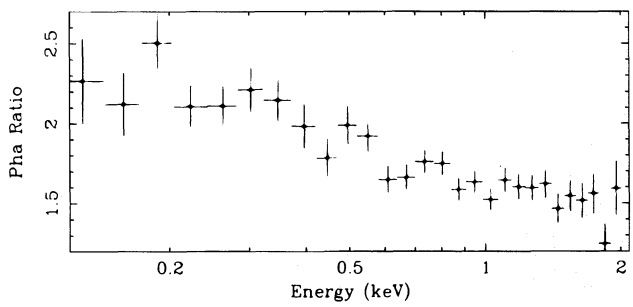

FIG. 3.—PHA ratios of *ROSAT* spectra showing that the spectrum from the 1991 observation is substantially softer than that from the 1992 observation.

3. SPECTRAL FITTING RESULTS

3.1. *The Ginga Data*

The 1988 data were accumulated into four spectra including the total spectrum as well as spectra from each day separately, while the 1989 data were accumulated into one spectrum. These spectra were fitted from 1.11 to 20.9 keV with an absorbed power law plus Gaussian emission-line model, with the line energy fixed to 6.4 keV and width (σ) fixed to 0.05 keV. The parameters from these fits are listed in Table 1, with the line flux in column (4) and the line equivalent width in column (5). All fits were acceptable, except for G88.1, where the poor fit can be partially attributed to the lowest energy channels. Ignoring an additional lowest two channels results in an acceptable fit ($\chi^2_\nu = 1.25$), with no significant difference in continuum fit parameters. The absorbing column densities are generally consistent with the Galactic value; note that columns below 10^{21} cm^{-2} cannot be determined using *Ginga*. The apparent photon index is variable and clearly correlated with the flux, as suggested by the hardness ratios shown in Figures 1*a* and 1*b*. The line flux does not vary significantly, although there is the suggestion of a decrease in line flux in the lower flux spectrum from 1989. The equivalent width appears to increase, but the change is not significant.

3.1.1. *Reflection Model Fitting*

The reflection model has been shown to describe *Ginga* spectra from Seyfert 1 galaxies well (e.g., Nandra & Pounds 1994). Two scenarios represent the extremes of variability behavior in the reflection model, and these can be used to place constraints on observed spectral variability (e.g., George et al. 1993). If the reflecting material is either far from the central engine or extends far from the central engine compared with the variability timescale, the

TABLE 1

PARAMETERIZING MODEL FIT RESULTS

Spectrum (1)	N_H (10^{21} cm^{-2}) (2)	Photon Index (3)	P1[a] (4)	P2[b] (5)	Flux (10^{-11} ergs cm^{-2} s^{-1})[c] (6)	χ^2/dof (7)
G88.tot.....	<0.3	$1.81^{+0.02}_{-0.01}$	$5.2^{+1.9}_{-1.6}$	130^{+50}_{-40}	4.1	30/29
G88.1.....	<0.8	$1.85^{+0.05}_{-0.02}$	$5.2^{+2.7}_{-2.6}$	110^{+60}_{-50}	4.8	47/29
G88	<0.4	$1.77^{+0.03}_{-0.02}$	$5.2^{+2.7}_{-2.3}$	140^{+70}_{-60}	3.5	21/29
G88.3.....	<0.7	$1.77^{+0.03}_{-0.02}$	$5.2^{+2.7}_{-2.3}$	130^{+70}_{-60}	3.8	22/29
G89.2.....	$0.4 < 3.3$	$1.58^{+0.10}_{-0.07}$	$3.9^{+3.1}_{-2.9}$	180^{+140}_{-130}	2.0	25/29
R91.....	$0.67^{+0.04}_{-0.03}$	2.4 ± 0.1	$0.85^{+0.09}_{-0.10}$	0.27 ± 0.13	3.4	22/25
R92.....	0.57 ± 0.2	2.2 ± 0.1	$0.92^{+0.06}_{-0.07}$	0.28 ± 0.09	2.0	11/25

[a] Additional model parameter. For the *Ginga* spectra, this is the narrow (0.05 keV) line flux ($\times 10^{-5}$ photons cm^{-2} s^{-1}) at fixed energy 6.4 keV, and for the *ROSAT* spectra it is the energy of the absorption edge (keV).

[b] Additional model parameter. For the *Ginga* spectra, this is the equivalent width of the 6.4 keV iron line measured in eV, and for the *ROSAT* spectra it is the optical depth of the edge.

[c] For Ginga, this is the 2–10 keV flux, while for *ROSAT* it is the 0.1–2 keV flux.

response of the reflecting material would be lagged and smeared, and this would be observed as a constant normalization of the reflected component. The following model expresses the reflection component normalization explicitly:

$$F(E) = e^{-\sigma(E)N}[N_\Gamma E^{-\Gamma} + N_{\rm refl} A(E, \Gamma) + I_L(E)] . \quad (1)$$

$A(E, \Gamma)$ is the reflection spectrum for a face-on orientation, and $I_L(E)$ is the Gaussian expression for the iron Kα fluorescence line, with energy and σ fixed as before. In contrast, if the reflection region is small compared with the source variability timescale, the ratio between the normalization of the reflection component and the power-law component referred to as the reflection ratio r should be constant. The following model expresses the reflection ratio explicitly:

$$F(E) = e^{-\sigma(E)N}\{N[E^{-\Gamma} + rA(E, \Gamma)] + I_L(E)\} . \quad (2)$$

A face-on orientation with the reflecting material subtending a solid angle $\Omega = 2\pi$ to the primary hard X-ray emission is implied when $r = 1$.

The fit results to both models are given in Table 2. Piro et al. (1990) previously analyzed the average spectrum from the 1988 observation; our results are consistent with theirs, and the smaller fit χ^2_ν from this analysis probably reflects a more conservative data selection. The low flux of the 1989 observation resulted in poor statistics, so that the parameters of the reflection model could not be constrained. Overall, the values obtained for the reflection ratio are generally larger than 1, though most are consistent with 1 at the 90% confidence level. The ratio found for the spectrum G88.1, which has the highest flux and the softest spectrum, is the largest, in contrast with the expectation that it should be the smallest since a smaller contribution of the reflection would result in a softer spectrum. This is most likely due to the coupling of the photon index, absorption, and reflection ratio in the spectral fitting.

The parameterizing spectral fit results and hardness ratios show that the 1989 spectrum is significantly flatter than that from 1988. Assuming that the data can be described adequately by the model in equation (1), we can

TABLE 2

REFLECTION MODEL FITS TO SPECTRA

Spectrum	N_H (10^{21} cm^{-2})	Photon Index	N(power law)[a]	N(reflection)[a]	Reflection Ratio	Line Flux[b]	Equivalent Width (eV)	χ^2/dof
G88.tot.....	$1.3 < 3.1$	2.0 ± 0.1	$1.4^{+0.3}_{-0.2}$	$2.6^{+3.3}_{-1.6}$	$1.9^{+1.7}_{-1.1}$	$5.0^{+1.7}_{-1.8}$	120 ± 40	14/28
G88.1.....	$3.0^{+2.6}_{-2.0}$	2.1 ± 0.2	$2.0^{+0.6}_{-0.3}$	$5.7^{+10.2}_{-3.6}$	$2.9^{+3.1c}_{-1.6}$	$4.6^{+2.5}_{-2.6}$	90 ± 50	32/28
G88.2.....	$0 < 1.8$	1.9 ± 0.1	$1.0^{+0.2}_{-0.1}$	$1.3^{+2.3}_{-0.8}$	$1.2^{+2.0}_{-0.6}$	5.0 ± 2.4	140 ± 70	13/28
G88.3.....	$0 < 4.4$	$1.9^{+0.3}_{-0.1}$	$1.2^{+0.4}_{-0.6}$	$2.1^{+6.6}_{-1.7}$	$1.8^{+3.5}_{-1.3}$	$5.0^{+2.6}_{-2.5}$	130^{+70}_{-60}	16/28
G89.....	$2.2 < 13.0$	$1.7^{+1.2}_{-0.2}$	$0.5^{+1.0}_{-0.1}$	$0 < 60$	$0 < 6^c$	4.0 ± 3.0	180 ± 140	24/28
Joint fit.....	...	$1.96^{+0.09}_{-0.08}$	...	$2.4^{+1.7}_{-1.1}$	...	4.6 ± 1.5	...	39/57
G88.tot.....	$1.1 < 2.5$	...	$1.4^{+0.2}_{-0.1}$	...	$1.8^{+1.5}_{-0.9}$	...	110 ± 40	14
G89.....	$5.6^{+2.2}_{-2.1}$	...	$0.64^{+0.06}_{-0.05}$	...	$3.8^{+2.2c}_{-1.7}$	...	210 ± 70	25
Joint fit.....	$1.7^{+1.6}_{-1.3}$	$2.00^{+0.13}_{-0.10}$	...	...	...	...	...	66/85
G88.1.....	...	...	$1.8^{+0.3}_{-0.2}$	$2.7^{+3.3}_{-1.8}$	$1.6^{+1.4}_{-0.9}$	$4.6^{+2.6}_{-2.3}$	100^{+60}_{-50}	34
G88.2.....	...	...	$1.2^{+0.2}_{-0.1}$	$3.4^{+2.8}_{-1.6}$	$2.9^{+1.7}_{-1.2}$	$5.0^{+2.3}_{-2.6}$	130^{+60}_{-70}	16
G88.3.....	...	...	1.3 ± 0.2	$3.5^{+3.0}_{-1.7}$	$2.7^{+1.7}_{-1.1}$	$5.1^{+2.4}_{-2.7}$	120 ± 60	17

NOTES.—In the second and third panels, parameters from simultaneous fits of spectra are given. In the top row in each case the values of parameters constrained to be equal are listed, and in the succeeding rows the values of parameters left free and corresponding to each spectrum are listed.

[a] Model normalization ($\times 10^{-2}$ photons keV^{-1} cm^{-2} s^{-1} at 1 keV).

[b] Line flux ($\times 10^{-5}$ photons cm^{-2} s^{-1}) in the line.

[c] Parameter upper limits constrained by the table model limits.

test the hypothesis that variability in a single model parameter dominates the spectral variability by fitting the 1989 spectrum and the average 1988 spectrum simultaneously, tying most parameters together, and allowing various parameters to vary independently in turn. Doing so shows that variation in the absorption rather than the reflection ratio or the index produces the largest reduction in χ^2 (from 48/59 degrees of freedom [dof] to 38/55 dof). These results are given in the second part of Table 2, and the χ^2 contours computed for the absorption and index are shown in Figure 4. These show that long-term spectral variability assuming fixed reflection ratio is present at the 90% confidence level and can be modeled by a constant index but a change in absorption.

The hardness ratio shown in Figure 1*a* shows that the significant spectral variability occurring during the 1988 observation can be characterized by a change in ratio between the medium-energy band dominated by the power-law continuum and the hard energy band in which the reflection component contributes substantially. The character of the spectral variability suggests that either a change in index or reflection ratio has occurred. Fitting all three spectra simultaneously and requiring the spectral shape to stay the same with only a change in total normalization to account for the flux change gives $\chi^2 = 87.8/87$ dof. Again assuming that the spectral variability is dominated by variability of only one parameter, fitting with equation (2) shows that allowing either the photon index or reflection ratio to vary gives an equally good fit ($\chi^2 = 66/86$ dof). The χ^2 contours of spectra from the first and second days are shown in Figure 5, illustrating that the spectral variability can be explained by either a variable index or variable reflection ratio. Variability in the absorption explains the spectral variability less well ($\chi^2 = 78/86$ dof). Assuming it is the reflection ratio rather than the photon index that changed, fitting with the model described in equation (1) but allowing only the power-law normalizations to vary independently shows that these data are consistent with the reflection flux having remained constant during the 3 days of observation ($\chi^2 = 69/90$ dof).

The ambiguity of these results is inherent in *Ginga* data from moderate-flux Seyfert 1 galaxies, because the decrease

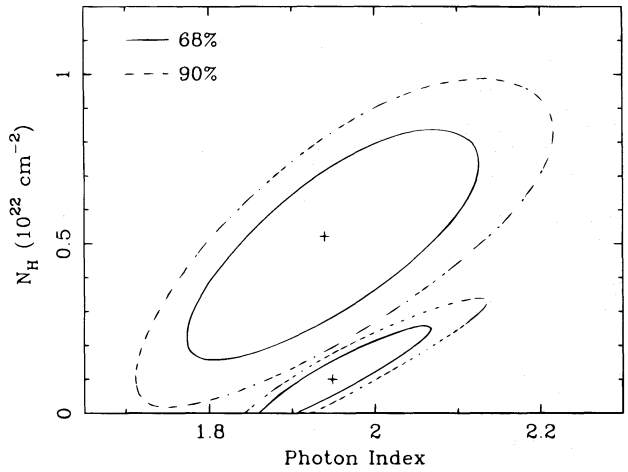

FIG. 4.—χ^2 contours (90% and 1 σ) for the average 1988 *Ginga* spectrum and the 1989 *Ginga* spectrum for a joint fit of the reflection model, allowing the index and absorption to vary. These show that in the context of the reflection model, the spectral variability can be explained by variation in the neutral absorption column.

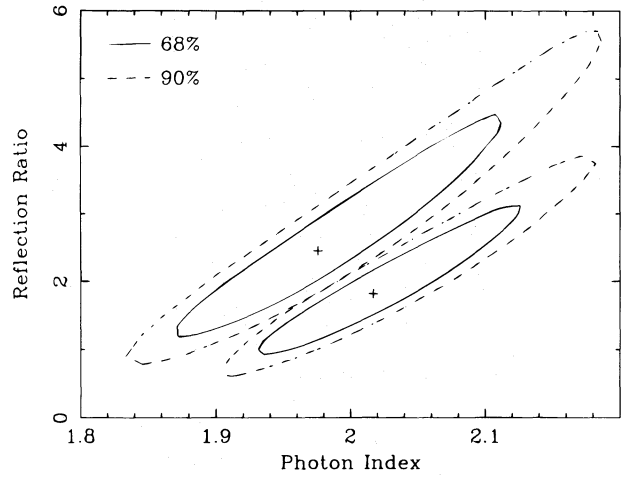

FIG. 5.—χ^2 contours (90% and 1 σ) for *Ginga* spectra G88.1 and G88.2 from a joint fit of the reflection model, allowing the index and reflection ratio to vary. These show that in the context of the reflection model, the spectral variability can be attributed to variability in the ratio or the index or both.

in detector effective area toward low energies means that the photon index in the reflection model is not well determined. Recent *ASCA* results may provide a partial precedent for the assumption that the spectral variability in this case was produced by a change in the reflection ratio rather than in the power-law index. During a 3 day *ASCA* observation of NGC 7469 in 1993, both 30% total flux variability and spectral variability was observed (Guainazzi et al. 1994), but spectral variability was confined to lower energies inaccessible to *Ginga*, while the power-law index determined above 2.5 keV remained constant. Note that large changes in the photon index are detectable in *ASCA* spectra, as shown in other observations of Seyfert 1 galaxies (e.g., Mrk 766; Leighly et al. 1996).

3.1.2. *Partial Covering Fits to Ginga Spectra*

It was shown by Piro et al. (1990) that the 1988 *Ginga* spectrum could be modeled by partial covering by a thick absorber. This model fit acceptably all the Ginga spectra separately, although for the 1989 data, the covering fraction could not be constrained. This model could potentially explain the observed variability because if the intrinsic emission were constant, an increase in the fraction covered would result in a decrease in observed emission as well as an overall hardening of the spectrum. Fitting the three 1988 *Ginga* spectra simultaneously and allowing only the covering fraction to vary independently gave a statistically acceptable fit ($\chi^2 = 78/87$ dof) with the covering fraction varying from 0.098 during the first day to 0.37–0.32 during the second and third days. However, determining the contribution to the total χ^2 from each spectrum separately shows that this fit was unacceptable for the spectrum from the first day ($\chi_\nu = 1.56/27$ dof). Allowing the partial covering column density to vary also did not result in a significant improvement in fit. Thus, if partial covering by neutral material is the cause of the flux and spectral variability, the intrinsic luminosity is required to vary in concert with the covering fraction, an unlikely scenario.

3.2. *The ROSAT Data*

The hardness ratios shown in Figure 2 and the PHA ratio shown in Figure 3 demonstrate that spectral variability occurred between the two *ROSAT* observations, but not

during each observation. Accumulating the data from each observation and fitting with a single absorbed power law from 0.1–2.0 keV reveals evidence for spectral complexity (R91: $\chi^2_\nu = 1.41/27$ dof; R92: $\chi^2_\nu = 1.61/27$ dof; see also Turner et al. 1993a, Brandt et al. 1993). Addition of an absorption edge, shown to be generally appropriate for *ROSAT* spectra from Seyfert 1 galaxies (e.g., Turner et al. 1993a), improves the fit substantially (Table 1). The column densities were consistent with each other and were slightly larger than the Galactic value of 4.8×10^{20} cm^{-2} (Elvis, Lockman, & Wilkes 1989). The photon indices were significantly different, much larger than those found in the *Ginga* spectra, and they were correlated with flux as suggested by the softness ratios in Figures 2*a* and 2*b*. The absorption edge energies, consistent with absorption by highly ionized oxygen, and optical depths were not well determined and are consistent with each other.

It is well known that some time-dependent residual uncertainty in the PSPC calibration remains. Although the gain change is a nonlinear function of energy, the change in gain seems to be a linear trend with time (*ROSAT* bulletin 64). These observations were made just 6 months apart, suggesting that the gain change between them should not be large. Further, the systematic error should be no larger than the difference between the two currently released *ROSAT* PSPC-B (Position Sensitive Proportional Counter) detector response matrices (referred to as "gain1" and "gain2"). Thus, the effect of a possible gain change can be tested by fitting each spectrum using the two different matrices simultaneously. Doing so using the above model and computing the χ^2 contours shows that model parameters are consistent for the two matrices but still differ significantly between the two spectra. Thus, the spectral variability observed between the two *ROSAT* spectra cannot be attributed to the residual uncertainty in the PSPC calibration.

3.2.1. *Soft Excess Modeling*

When a blackbody is used to model the spectral complexity (Table 3), the resulting power-law indices of 1.8–2.0 are consistent with the mean for Seyfert 1 galaxies found after reflection is accounted for (Nandra & Pounds 1994); in contrast, this model could not explain the *ROSAT* spectrum from NGC 3783, as the resulting extremely flat index was considered physically implausible (Turner et al. 1993b). The absorption becomes pegged at the Galactic value in the spectral fitting of the 1992 data, possibly an indication that the soft excess component is broader than a single blackbody (e.g., NGC 5548; Done et al. 1995). Fitting with an additional blackbody results in a reduction in χ^2 by 7.3 with a reasonable absorption column ($N_{\rm H} = 5.4 \times 10^{20}$ cm^{-2}) but a flatter index which could no longer be constrained. The absorption, photon index, and blackbody temperature are consistent between the two *ROSAT* spectra. Fitting jointly and leaving only the continuum normalizations free gave a good fit ($\chi^2 = 50/50$ dof) suggesting that most of the observed spectral variability can be explained by a change in relative normalization between the power law and the blackbody component. Allowing any of the three other parameters to vary independently resulted in a better fit ($\chi^2 = \sim 35/49$ dof for all three), but because of the poor energy resolution and limited bandpass of the PSPC, it cannot be determined which parameter further contributes to the spectral variability.

3.2.2. *Warm Absorber Model Fits*

The *ROSAT* spectra can be successfully fit using a model which includes an edge presumably resulting from absorption by partially ionized material in the line of sight. The ionization state of the material can be described by the ionization parameter $U = Q/4\pi r^2 c N_e$, where Q is the flux of ionizing photons, r is the distance from the source of ionizing radiation, and N_e is the density of the ionized gas (Yaqoob, Warwick, & Pounds 1989). The photonized gas in the line of sight should respond to continuum flux changes resulting in spectral variability (e.g., Halpern 1984). Generally speaking, due to reduced soft X-ray opacity *ROSAT* spectra should be observed to soften as the flux increases, and the measured edge energy may increase correlated with the dominant ionization state of oxygen. In *Ginga* data, in which the lower end of the bandpass is significantly above the oxygen edge energies, the primary result is an apparent correlation between absorption and flux (e.g., Nandra, Pounds, & Stewart 1990).

Spectral fitting was done using a warm absorber table model (Yaqoob et al. 1989). Fitting the two *ROSAT* spectra separately showed that the photon indices are consistent while the log (U) and log ($N_{\rm warm}$) values vary marginally such that the ionization parameter is correlated with the flux. The results are given in Table 4. Assuming that the index is constant allows tighter constraints on remaining parameters, showing that the ionization parameter and ionized column increase while the neutral absorption decreases as the flux increases. Note that there is still strong coupling of the three remaining parameters, and given the low resolution of the PSPC spectra, these results are highly model dependent.

3.3. *The Ionized Disk Model*

The hard X-ray tail observed in *Ginga* spectra is thought to result from scattering of incident primary X-rays by an accretion disk. If the reflection region is close to the nucleus, the disk surface material may become ionized, resulting in reflection at soft X-ray energies due to reduced opacity to soft X-rays. Emission lines should also be produced through recombination. This model without accounting for line emission was used to explain the X-ray spectrum of Cyg X-1 by Done et al. (1993). Ionized disk models accounting for line emission have been developed by Ross & Fabian (1993) and Zycki et al. (1994).

TABLE 3

BLACKBODY MODEL FIT RESULTS

Spectrum	$N_{\rm H}$ (10^{21} cm^{-2})	Photon Index	N(power law)[a]	$kT_{\rm bb}$ (keV)	N(blackbody)[b]	χ^2/dof
R91	$0.5 < 0.6$	$2.0^{+0.4}_{-0.3}$	$1.17^{+0.13}_{-0.06}$	$0.10^{+0.01}_{-0.02}$	$2.1^{+0.9}_{-0.8}$	22/24
R92	Galactic < 0.53	$1.8^{+0.2}_{-0.1}$	$0.70^{+0.05}_{-0.02}$	0.11 ± 0.01	1.1 ± 0.2	10/24

[a] Power-law normalization ($\times 10^{-2}$ photons keV^{-1} cm^{-2} s^{-1} at 1 keV).
[b] Blackbody component normalization ($\times 10^{-4}$ ergs cm^{-2} s^{-1}).

TABLE 4

WARM ABSORBER MODEL FIT RESULTS

Spectrum	N_H (10^{21} cm^{-2})	Photon Index	log U	log N_{warm}	χ^2/dof
Index free:					
R91	$0.53^{+0.08}_{-0.06}$	$2.2^{+0.4}_{-0.2}$	$0.4 < 0.6$	$22.7 < 23.2$	23/24
R92	$0.59^{+0.03}_{-0.04}$	2.2 ± 0.1	$0.2^{+0.1}_{-0.4}$	$22.3^{+0.4}_{-0.8}$	9/24
Index constrained:					
R91	$0.51^{+0.05}_{-0.02}$	$2.1^{+0.2}_{-0.1}$	0.4 ± 0.1	$22.9^{+0.3}_{-0.5}$	23/25
R92	0.58 ± 0.03	...	$0.2^{+0.1}_{-0.4}$	$22.4^{+0.3}_{-1.0}$	10/25

TABLE 5

IONIZED DISK FIT RESULTS

Spectrum	N_H (10^{21} cm^{-2})	Photon Index	ξ	Ratio	χ^2/dof
G88.tot.....	$1.5^{+1.1}_{-1.4}$	$2.05^{+0.05}_{-0.08}$	$23 < 137$	1.7 ± 0.7	13/24
R91.....	$0.66^{+0.16}_{-0.05}$	2.3 ± 0.2	100^{+80}_{-90}	$2.1^{+3.2}_{-1.0}$	23/24
R92.....	$0.68^{+0.09}_{-0.04}$	2.1 ± 0.1	100^{+40}_{-70}	$2.0^{+1.5}_{-0.8}$	14/24

We use the model developed by Zycki et al. (1994) for spectral fitting parameterized by the ionization parameter $\xi = 4\pi F/n$, where F is the integrated ionizing flux and n is the number density. Results are given in Table 5. The 1988 *Ginga* spectrum could not constrain the ionization parameter, so it was consistent with reflection from neutral material. The ionization parameter could be constrained by the *ROSAT* spectra, primarily because of the spectral com-

TABLE 6

JOINT *ROSAT* AND *Ginga* SPECTRAL FIT RESULTS

A. WARM ABSORBER

Spectrum	N_H (10^{21} cm^{-2})	Photon Index	Reflection Ratio	Line Flux[a]	EW (eV)	log U	log N_{warm}	χ^2/dof
Warm absorber:								
Joint	0.53 ± 0.03	$2.17^{+0.06}_{-0.05}$	...	...	...	$0.4^{+0.2}_{-0.1}$	$22.6^{+0.3}_{-0.2}$	41/49
G88.tot	...	...	$3.5^{+1.1}_{-0.9}$	$2.9^{+1.8}_{-1.9}$	60 ± 40	...	...	17
R91	...	...	...	...	...	...	...	24
Joint	0.58 ± 0.02	2.13 ± 0.04	...	...	...	0.2 ± 0.1	22.3 ± 0.2	24/49
G88.tot	...	...	$3.3^{+0.9}_{-0.8}$	$3.9^{+1.6}_{-2.1}$	90^{+40}_{-50}	...	...	14
R92	...	...	...	...	...	...	...	10

B. IONIZED DISK

Spectrum	N_H (10^{21} cm^{-2})	Photon Index	Reflection Ratio	ξ	χ^2/dof
Joint.....	$0.64^{+0.07}_{-0.04}$	$1.97^{+0.06}_{-0.04}$	...	120^{+40}_{-50}	48/50
G88.tot.....	...	...	$1.2^{+0.5}_{-0.2}$	...	15
R91.....	...	...	$4.6^{+1.4}_{-1.3}$	...	33
Joint.....	0.67 ± 0.04	2.00 ± 0.04	...	110 ± 40	33/50
G88.tot.....	...	...	$1.3^{+0.4}_{-0.3}$	...	15
R92.....	...	...	$2.79^{+1.05}_{-0.69}$	...	18

C. BLACKBODY

Spectrum	N_H (10^{21} cm^{-2})	Photon Index	Reflection Ratio	Line Flux[a]	EW (eV)	kT	Normalization[b]	χ^2/dof
Joint.....	Galactic < 0.5	$1.92^{+0.04}_{-0.01}$	...	...	...	...	...	38/53
G88.tot.....	...	...	$1.5^{+0.6}_{-0.2}$	4.9 ± 1.7	120 ± 40	...	...	15
R91.....	...	...	...	...	...	$0.10^{+0.004}_{-0.007}$	$2.5^{+0.5}_{-0.3}$	23
Joint.....	$0.51^{+0.03}_{-0.02}$	1.91 ± 0.04	...	...	...	...	...	26/53
G88.tot.....	...	...	$1.4^{+0.6}_{-0.5}$	4.9 ± 1.7	120 ± 40	...	...	15
R92.....	...	...	...	...	...	0.11 ± 0.01	0.9 ± 0.2	11

NOTES.—In the second and third panels, parameters from simultaneous fits to spectra are given. In the top row in each case the values of parameters constrained to be equal are listed, and in the succeeding rows the values of parameters left free and corresponding to each spectrum are listed. Note that the iron line is already included in the ionized disk model so no separate line flux is given.

[a] Line flux ($\times 10^{-5}$ photons cm^{-2} s^{-1}) in the line.

[b] Blackbody normalization in units of $L_{39}/(D_{10})^2$, where L_{39} is the source luminosity in units of 10^{39} ergs s^{-1}, and D_{10} is the distance to the source in units of 10 kpc.

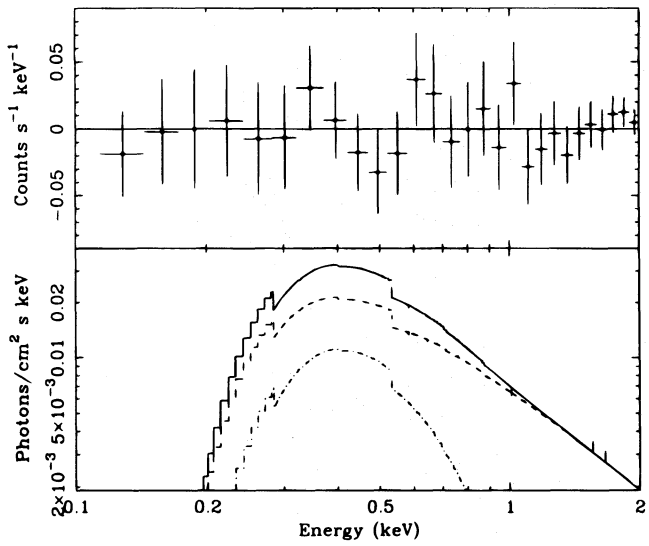

FIG. 6a

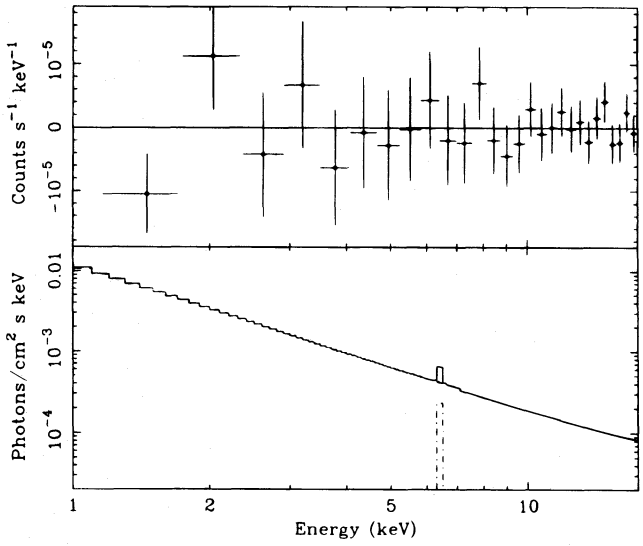

FIG. 6b

FIG. 6.—Fit residuals plus model for the joint fit of the power law–blackbody–reflection-line model to the nonsimultaneous *ROSAT* and *Ginga* spectra. (*a*) 1992 *ROSAT*; (*b*) 1988 *Ginga*.

plexity. The resulting photon index for the 1992 spectrum was consistent with the *Ginga* result but was significantly larger for the 1991 spectrum. The ratio of the reflected to the incident flux indicates that more than half the incident flux must be reprocessed by the ionized material.

3.4. *Joint Model Fits*

The complexity of the broadband spectrum makes development of a coherent model for the emission and variability of NGC 7469 difficult when spectra from each mission separately cover only a limited energy band. An attempt is made to develop a coherent model by fitting together the nonsimultaneous *ROSAT* and *Ginga* spectra to the models investigated above. This procedure is justified if we assume that the photon index does not change and that we have modeled correctly the spectral variability in the *Ginga* data with a variable reflection ratio. These results are given in Table 6; in the first row of each group, the values from parameters tied together are given along with the total χ^2, while subsequent rows display the parameters specific to each spectrum and the contribution from that spectrum to the total χ^2. Since all the models gave good fits, they must be distinguished by whether the fit parameters are physically reasonable.

Fitting the spectra with a power law plus reflection and warm absorber model gives the results in the first section of Table 6. Reasonable values of log (U) and log ($N_{\rm warm}$) constrained primarily by the *ROSAT* spectra are found; however, the *ROSAT* spectra force a steep photon index to fit the warm absorber, which is compensated for in the *Ginga* spectrum by an unphysically large reflection normalization ratio. Further, the intrinsic index is required to be $\sim$2.2, which is rather more steep than that generally found from Seyfert 1 galaxies (e.g., Nandra & Pounds 1994). Thus, the warm absorber alone does not describe the complex soft X-ray spectrum of NGC 7469 well. Note that no evidence for a warm absorber was found in the higher resolution spectrum from the 1993 *ASCA* observation of NGC 7469 (Guainazzi et al. 1994).

The parameters of the ionized disk model obtained for the *ROSAT* and *Ginga* spectra when fitted separately as shown in Table 4 are mostly consistent with one another, except for the ratio of reflected emission. Fitting the spectra together and allowing the ratio to vary independently gives consistent results; however, the fits to the *ROSAT* spectra are somewhat worse than for other combined model fits. This is because the ionized reflection spectrum is dominated by soft X-ray lines rather than the steep soft X-ray continuum required to fit the *ROSAT* spectra.

Modeling the soft component using a single-temperature blackbody produced a good fit to the *ROSAT* and *Ginga* spectra together. In both cases, the photon index was about 1.9, reasonable for Seyfert 1 galaxies (e.g., Nandra & Pounds 1994), and the column density was near the Galactic value. The reflection ratios were slightly higher than 1, but this may be expected since the average 1988 *Ginga* spectrum was used. The line equivalent width of $\sim$120 eV is consistent with production in an accretion disk or other cold extended material (e.g., George & Fabian 1991; Sivron & Tsuruta 1993; Krolik, Madau, & Zycki 1994). The blackbody temperature of $\sim$110 eV was consistent between the two *ROSAT* spectra, while the flux varied by nearly a factor of 3 in this parameterization. Uncorrelated variability between the soft excess and power-law continua normalizations was also found in the 1993 *ASCA* observation (Guainazzi et al. 1994). The residuals and model shown in Figure 6 are given for the 1992 *ROSAT* and the 1988 *Ginga* spectra. The soft excess could also be modeled equally well by a multiple blackbody accretion disk spectrum, requiring a slightly higher column density and temperature, but the uncertainties in the normalization for this parameterization indicate no significant change in flux between the two *ROSAT* observations, showing that soft excess variability is model dependent.

4. DISCUSSION

4.1. *Constraints on the Origin of the Hard X-Ray Reflection*

The significant spectral variability found in the 1988 *Ginga* observation could be attributed to either a variable photon index or a variable ratio of reflected to primary emission. If the photon index is assumed not to have varied

over the 3 day period, then the reflection ratio must have changed in order to produce the spectral variability. The reflection flux is consistent with a constant value; the assumption that it was constant leads to constraints on the location of the reflection region.

One attractive explanation for the observed spectral variability is that much of the reflecting material is located at least 3 light days from the source, and so that contribution can be determined. Two different scenarios must be considered, since the reflection ratio measured on the first day was larger than 1. That value of the reflection ratio might correspond to the physical reflection ratio, implying that the reflecting material subtends a correspondingly larger solid angle than 2π sr. Given the change in intrinsic emission, a constant reflection flux would imply a reflection ratio for the second and third day of about 0.6, implying that at least 40% of the reflected emission must come from farther than 3 light days from the center. On the other hand, it could be that the physical reflection ratio is 1, implying that the intrinsic X-ray emission was larger before this observation. By the same reasoning, more than 60% should be coming from a region more than three light days from the central region.

Matt, Perola, & Piro (1991) show that for a source located $20r_s$ above the disk, for inner and outer disk radii of 10 and $1000r_s$, respectively, and moderate inclination, half the reflected photons must come from the inner $\sim 50r_s$. For a lag of 3 light days, these limits imply a black hole mass of $\sim 5 \times 10^8\ M_\odot$. If the source is confined within $6r_s$, the light crossing time is about 30,000 s. The light curve shown in Figure 1*b* and also the light curve shown in Figure 1 of Barr (1986) indicate that the doubling timescale is about 7 hr, just within this limit. Thus, the variability timescales indicate that it is just possible that the observed constant reflected emission could have come from the relativistic disk. An alternative site for the reflection is the molecular torus, hypothesized to lie outside the broad-line region. Recent modeling by Ghisellini, Haardt, & Matt (1994) and Krolik et al. (1994) demonstrates that an iron fluorescence line and reflection hump can be produced, very similar to those found from a source located above a flat accretion disk, the geometry considered by Matt et al. (1991) and others.

The profile of the iron Kα line, which should also be produced in the material responsible for the reflection, can be used to distinguish between these two origins. Both the relativistic accretion disk and material further away such as a molecular torus are expected to produce a line of ~ 100 eV equivalent width when illuminated by a hard X-ray continuum (e.g., George & Fabian 1991; Krolik et al. 1994). If the iron line is produced in the relativistic accretion disk the profile should be broadened by gravitational and Doppler effects (e.g., Matt et al. 1991), while if the line is produced in the molecular torus, the line should be narrow. The *ASCA* spectrum of NGC 7469 had a narrow iron Kα line with $\sigma < 150$ eV (Guainazzi et al. 1994). This contrasts with the *ASCA* spectra of many Seyfert 1 nuclei, which contain clearly broad lines (e.g., Mushotzky et al. 1995). In the long observation of MCG -6-30-15, the line profile clearly suggested emission from a relativistic accretion disk (Tanaka et al. 1995). Thus, the observed narrow line in NGC 7469 provides further evidence that the reflection comes from a more extended region. An equivalent width change corresponding to the reflection ratio change is also expected, but it cannot be constrained with these data.

The lack of change in the reflection component flux was suggested by observed spectral variability in *Ginga* data from two other Seyfert 1 nuclei: Mrk 841 (George et al. 1993) and NGC 5548 (Nandra et al. 1991). In both these cases, though, the interval between the observations was far too long to place any useful constraint on the geometry.

4.2. *The Temperature of the Thermal Component*

The soft excess component in the *ROSAT* data was described most successfully by thermal models. The temperatures found ranged between 100–110 eV for a single blackbody and ~ 140 eV for the inner edge temperature of the multiple blackbody accretion disk spectrum. The blackbody temperature for the soft excess component in the *ASCA* spectrum was found to be 80(66, 99) eV (Guainazzi et al. 1994). These temperatures may be slightly high to be the emission from a bare accretion disk (e.g., Ross, Fabian, & Mineshige 1992), but they are consistent with those observed in *ROSAT* spectra from other Seyfert 1 nuclei with similar luminosity (e.g., Walter & Fink 1993).

When the *ROSAT* and *Ginga* data were fitted simultaneously with a power law, reflection, and blackbody model, it was found that the spectral variability in the *ROSAT* data could be explained by a change in the relative normalization between the blackbody component and the power law, so that the softer brighter *ROSAT* spectrum could be explained by the greater relative contribution of the soft excess component. In the *ASCA* observation, the spectrum was found to soften with an increase in flux, implying that the variability of the two components was not correlated (Guainazzi et al. 1994). Two-component spectral behavior was also found in the *EXOSAT* data, where the 1–7 keV X-rays varied significantly while the 0.05–2 keV energy X-rays remained constant (Barr 1986), which has been subsequently explained by a constant thermal component (Walter & Courvoisier 1992). These results may imply that thermal reprocessing of primary X-rays in accretion disk material, posited to explain correlated variability found in the UV-optical bands from some Seyfert 1 galaxies (e.g., Clavel et al. 1992), is relatively less important on long timescales in this object and could be further evidence that hard X-ray reprocessing does not occur primarily in the inner disk.

4.3. *The Absorbing Material*

We found that the best explanation for the flatter spectrum of the 1989 *Ginga* observation was a change in the neutral absorption. Although the statistics were poor, this result is interesting, since similar inverse correlations of absorption with flux have been seen between *Ginga* observations of other Seyfert 1 galaxies, including Mrk 335 (Turner et al. 1993c).

Barr (1986) noted that because of the large reddening seen in the stellar spectrum and narrow line emission, the soft excess in the *EXOSAT* spectra may be much larger than measured. The reddening of $E(B-V) = 0.3$ would correspond to a neutral absorption column of $N_{\rm H} = 1.8 \times 10^{21}$ cm^{-2} assuming a standard dust-to-gas ratio. The low bandpass of *ROSAT* allows precise measurement of the absorption column, especially considering the good statistics of the spectrum from 1992. Although the model for the soft component is uncertain, none of the models considered here required a neutral absorption column of more than 7×10^{20} cm^{-2}, less than one-third of the column esti-

mated from reddening. Thus, there is no evidence that gas corresponding to the optical reddening covers the nucleus. Alternatively, a gas-to-dust ratio approximately 3 times Galactic may be implied.

A warm absorber can explain the *ROSAT* spectra alone, but it is less successful in explaining the combined *ROSAT* and *Ginga* spectra. Further, in the higher energy resolution *ASCA* spectrum, no evidence for a warm absorber was found (Guainazzi et al. 1994). This result contrasts with those from other *ASCA* observations of Seyfert 1 galaxies which find soft X-ray edges explained by absorption through partially ionized material to be common (e.g., MCG −6-30-15; Fabian et al. 1994; Otani 1995). However, repeated observations using *ASCA* show that the column density of the warm absorber is sometimes variable (Fabian et al. 1994), so that the lack of observation of a warm absorber during a single observation does not preclude its existence. It is possible that the larger neutral absorption column discovered in the 1991 *Ginga* observation could be the signature of a warm absorber (e.g., Nandra et al. 1990), with the statistics of the spectrum being too poor to detect the ionized iron absorption edge. Further, the 40% flux variability observed in 12 hr during the 1992 *ROSAT* observation with no accompanying spectral variability is probably consistent with the warm absorber model, since it would be difficult to measure fine changes in the model parameters considering the energy resolution and statistics, and since the ionization state may not change on timescales shorter than about 1 day. Other reasons why warm absorbers may not be observed to vary are explored in Turner et al. (1993b).

5. CONCLUSIONS

We have presented analysis of the *ROSAT* and *Ginga* observations of NGC 7469 in order to address the X-ray temporal and spectral variability. The most notable result is the detection of significant spectral variability in the hard X-rays occurring during the 1988 *Ginga* observation. Since the spectrum can be most successfully explained by a power law plus reflection model, to produce the observed spectral variability a change in either the power-law index or the reflection ratio must have occurred. Assuming that the power-law index did not change (an assumption based partially on the observed lack of change during an *ASCA* observation; Guainazzi et al. 1994), the reflection ratio must have changed. The reflection flux could not be well determined but is consistent with a constant value. This fact, plus the narrow rather than broad iron Kα line observed in the *ASCA* spectrum (Guainazzi et al. 1994) makes an extended origin for the reflection, for example, in the molecular torus, an attractive hypothesis.

Spectral variability was found between two *ROSAT* observations 6 months apart, which was clearly much more than would be produced from uncalibrated gain changes of the PSPC. The spectral complexity could be modeled by various soft components, including a blackbody and a warm absorber. Fitting nonsimultaneous *ROSAT* and *Ginga* spectra together, again under the assumption that the photon index had not changed, found the blackbody thermal component favored as the explanation for the soft excess. This explanation is supported further by the observation of a soft excess component and no ionized oxygen absorption edges in the *ASCA* spectrum (Guainazzi et al. 1994). The observed spectral variability could then be explained by a change in the relative normalization between the power-law and thermal components.

A common assumption in this analysis is that the photon index did not change. This assumption is necessary because of the limited bandpass of both the PSPC and the LAC. The ambiguity of determining the photon index in *Ginga* spectra will also be a problem in the analysis of X-Ray Timing Explorer (XTE) spectra from Seyfert 1 objects exhibiting reflection; however, this can be overcome successfully by coordinated observations with *ASCA* because of the increase in effective area toward low energies provided by *ASCA*. Coordinated monitoring experiments using *ASCA* and XTE provide also a good way to determine directly through variability whether the relativistic disk producing the broad line in other Seyfert 1 galaxies is also the origin of the reflection spectrum.

This research has made use of data obtained through the High Energy Astrophysics Science Archive Research Center Online Service, provided by the NASA-Goddard Space Flight Center. K. L. acknowledges helpful conversations with Richard Mushotzky, Tahir Yaqoob, and Mike Loewenstein. We thank the anonymous referee whose comments resulted in a great improvement of the paper. Part of the analysis was done at Nagoya University, and K. L. thanks the staff and graduate students for their hospitality. The warm absorber spectral fitting model was provided by Tahir Yaqoob, and the ionized disk model was provided by P. Zycki. K. L. acknowledges receipt of a National Research Council research associateship. S. T.'s and part of K. L.'s contributions were supported by NASA grants NAGW-2208, NAG 8-783, and NAG 5-1830. K. L.'s contribution was also partially supported by a 1993 *Ginga* Visiting Investigator Grant.

REFERENCES

Barr, P. 1986, MNRAS, 223, 29P
Brandt, W. N., Fabian, A. C., Nandra, K., & Tsuruta, S. 1993, 255, 996
Brinkmann, W., et al. 1994, A&A, 288, 433
Clavel, J., et al. 1992, ApJ, 393, 113
Done, C., Mulchaey, J. S., Mushotzky, R. F., & Arnaud, K. A. 1993, ApJ, 395, 273
Done, C., Pounds, K. A., Nandra, K., & Fabian, A. C. 1995, MNRAS, 275, 417
Elvis, M., Lockman, F. J., & Wilkes, B. J. 1989, AJ, 97, 777
Fabian, A. C., et al. 1994, PASJ, 46, L59
Fiore, F., Elvis, M., McDowell, J. C., Siemiginowska, A., & Wilkes, B. J. 1994, ApJ, 431, 515
Fiore, F., Perola, G. C., Matsuoka, M., Yamauchi, M., & Piro, L. 1992, A&A, 262, 37
Forman, W., Jones, C., Cominsky, L., Julien, P., Murray, S., Peters, G., Tananbaum, H., & Giacconi, R. 1978, ApJS, 38, 357
George, I. M., & Fabian, A. C. 1991, MNRAS, 249, 352
George, I. M., Nandra, K., Fabian, A. C., Turner, T. J., Done, C., & Day, C. S. R. 1993, MNRAS, 260, 111
Ghisellini, G., Haardt, F., & Matt, G. 1994, MNRAS, 267, 743
Grandi, P., Tagliaferri, G., Giommi, P., Barr, P., & Palumbo, G. G. C. 1992, A&AS, 82, 93
Guainazzi, M., Matsuoka, M., Piro, L., Mihara, T., & Yamauchi, M. 1994, ApJ, 436, L35
Halpern, J. P. 1984, ApJ, 281, 90
Hayashida, K., et al. 1989, PASJ, 41, 373
Krolik, J. H., Madau, P., & Zycki, P. T. 1994, ApJ, 420, 57
Leighly, K., Kunieda, H., Tsusaka, Y., Awaki, H., & Tsuruta, S. 1994, ApJ, 421, 69
Leighly, K., Mushotzky, R., Yaqoob, T., Kunieda, K., & Edelson, R. 1996, ApJ, in press
Leighly, K., Pounds, K., & Turner, T. J. 1989, in Proc. 23d ESLAB Symp., ed. J. Hunt & B. Battrick (Paris: ESA), 961
Marshall, N., Warwick, R. S., & Pounds, K. A. 1981, MNRAS, 194, 987

Matsuoka, M., Piro, L., Yamauchi, M., & Murakami, T. 1990, ApJ, 361, 440
Matt, G., Perola, G. C., & Piro, L. 1991, A&A, 247, 25
Mushotzky, R. F., et al. 1995, MNRAS, 272, 92
Nandra, K., & Pounds, K. A. 1994, MNRAS, 268, 405
Nandra, K., Pounds, K. A., & Stewart, G. C. 1990, MNRAS, 242, 660
Nandra, K., Pounds, K. A., Stewart, G. C., George, I. M., Hayashida, K., Makino, F., & Ohashi, T. 1991, MNRAS, 248, 760
Otani, C. 1995, Ph.D. thesis, Univ. Tokyo
Piro, L., Yamauchi, M., & Matsuoka, M. 1990, ApJ, 360, L35
Ross, R. R., & Fabian, A. C. 1993, MNRAS, 261, 74
Ross, R. R., Fabian, A. C., & Mineshige, S. 1992, MNRAS, 258, 189
Sivron, R., & Tsuruta, S. 1993, 402, 420
Tanaka, Y., et al. 1995, Nature, 375, 659
Turner, M. J. L., et al. 1989, PASJ, 41, 345
Turner, T. J., George, I. M., & Mushotzky, R. F. 1993a,, ApJ, 412, 72
Turner, T. J., Nandra, K., George, I. M., Fabian, A. C., & Pounds, K. A. 1993b, ApJ, 419, 127
Turner, T. J., et al. 1993c, ApJ, 407, 556
Turner, T. J., Weaver, K. A., Mushotzky, R. F., Holt, S. S., & Madejski, G. M. 1991, ApJ, 381, 85
Urry, C. M., Arnaud, K., Edelson, R. A., Kruper, J. S., & Mushotzky, R. F. 1989, in Proc. 23d ESLAB Symp., ed. J. Hunt & B. Battrick (Paris: ESA), 789
Walter, R., & Courvoisier, T. J.-L. 1992, A&A, 266, 65
Walter, R., & Fink, H. 1993, A&A, 274, 105
Weaver, K., Arnaud, K. A., & Mushotzky, R. F. 1995, ApJ, 447, 121
Yaqoob, T., Warwick, R. S., & Pounds, K. A. 1989, MNRAS, 236, 153
Zycki, P. T., Krolik, J. H., Zdziarski, A. J., & Kallman, T. R. 1994, ApJ, 437, 597